Green Vigilance: Drone Innovation for Early Detection of Crop Diseases

Erik Mischiatti, *233242*
Distribution Estimation for Robots and Vehicles *2023/2024*

***Abstract*—This study presents a simulation project aimed at enhancing plant condition monitoring in precision agriculture through the integration of Unmanned Aerial Vehicles (UAVs) and Unmanned Ground Vehicles (UGVs). The primary objective is the early detection of plant diseases using a distributed system for data analysis and communication between UAVs and UGVs. The UAV first conduct an aerial survey of the agricultural field, gathering data which is later analyzed to identify areas of interest. This data is then communicated to the UGVs, which are subsequently deployed for more detailed ground-level inspection. A hybrid sensing model, combining elements of depth sensing and spatial scanning, is employed to accumulate 3D data over time, constructing a detailed spatial representation of the field. Furthermore, a Weighted Least Squares (WLS) algorithm is utilized to manage the positional relationships among UGVs and between UGVs and plants, ensuring precise navigation and obstacle avoidance. An Extended Kalman Filter (EKF) improves the accuracy of UAV tracking and navigation by integrating GPS and IMU data. The simulation generates two-dimensional heatmaps to visualize disease distribution, guiding ground vehicles to the affected areas. The results demonstrate how the integration of UAV and UGVs, combined with advanced data analysis, can potentially revolutionize agricultural monitoring practices, providing innovative solutions for sustainable crop management and reducing losses due to plant diseases.**

I. Introduction

OVER the last few years, precision agriculture has emerged as one of the most significant innovations in the agricultural sector, aiming to improve the efficiency, productivity, and sustainability of farming practices. This discipline leverages advanced technologies to monitor and manage crops with precision, thereby minimizing resource use and optimizing agricultural yield. Among the most transformative technologies employed in precision agriculture are Unmanned Aerial Vehicles (UAVs) and Unmanned Ground Vehicles (UGVs), commonly known as drones, which have demonstrated a wide range of applications in this field.

The adoption of drones in agriculture has seen exponential growth in recent years, primarily due to their ability to rapidly collect high-resolution data over large areas. UAVs are utilized for various purposes, including land mapping, crop health monitoring, irrigation management, the application of pesticides and fertilizers, and assessing damage caused by adverse weather events [1], [2], [3]. Their versatility and efficiency in data collection make them indispensable tools for modern farmers seeking to adopt more precise and informed agricultural practices.

In particular, drones have proven effective in detecting plant diseases, especially in crops such as grapes, citrus, and olives [4]. Traditionally, drones gather multispectral, thermal, and visible images, which are processed using advanced algorithms like Convolutional Neural Networks (CNNs) and Support Vector Machines (SVMs) to identify symptoms of diseases and support decision-making processes [4], [5]. However, the standard camera model can be limiting in large-scale field operations. To address these limitations, we adopt a hybrid sensing approach, combining depth sensing and spatial scanning to construct a detailed 3D map of the agricultural field over time. This system accumulates spatial data as UAVs and UGVs explore the field, enhancing disease detection capabilities.

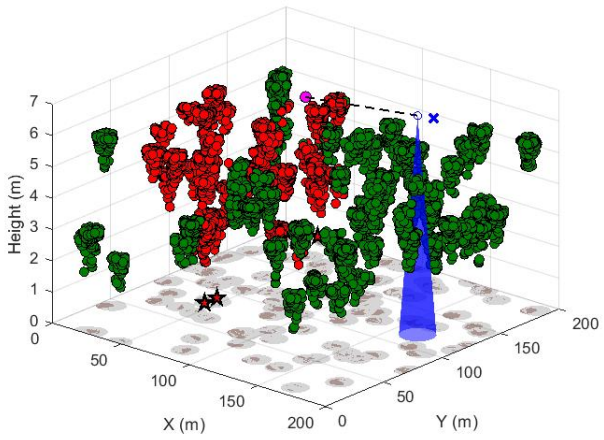

Fig. 1.

Despite the potential of these advanced sensing techniques, integrating drones with other agricultural systems, such as ground vehicles, remains a challenge due to the lack of standardized workflows and real-time data coordination [1], [3]. This highlights the need for more integrated and coordinated approaches in precision agriculture, which is a central focus of this work.

A crucial aspect of utilizing drones in precision agriculture is the accuracy of the collected data and the ability to integrate this information with other data sources to make informed decisions. This is where advanced data analysis algorithms, such as Weighted Least Squares (WLS) and Extended Kalman Filter (EKF), become essential.

The WLS method is a statistical technique that manages uncertainties in positioning and environmental data by assigning different weights to observations based on their reliability. This approach is particularly valuable in agricultural scenarios, where data can be affected by noise or unpredictable varia-

tions, thus improving the accuracy of analyses.

EKF, on the other hand, is an algorithm that extends the traditional Kalman Filter to handle nonlinear systems. In drone applications, EKF is employed to combine intermittent data from GPS and Inertial Measurement Units (IMU), thereby enhancing the accuracy of UAV tracking and navigation. This capability is crucial for ensuring reliable drone operations even in conditions of limited or interrupted GPS signals.

The integration of WLS and EKF in managing drones for precision agriculture represents a significant advancement, enabling farmers to obtain more accurate and actionable data to optimize crop management. These advanced data analysis tools are opening new possibilities for more efficient and sustainable agricultural management, reducing operational costs, and improving crop yields [2], [6].

The main objective of this work is to develop and simulate a distributed system using UAVs and UGVs to improve plant health monitoring in precision agriculture by detecting or not detecting the presence of diseases. By combining advanced data analysis techniques, such as WLS and EKF, with communication between airborne and ground-based units, and utilizing active sensing techniques to accumulate 3D data, this project aims to improve early detection of plant diseases, thus enabling timely and targeted interventions. The ultimate goal is to demonstrate how this approach can lead to more efficient and sustainable agricultural practices, reducing crop losses and optimizing the use of resources by demonstrating how the combined use of several agents with different characteristics can improve the overall outcome.

This paper is organised as follows:

Section II: Distributed System Architecture outlines the overall architecture of the proposed system, including the integration and coordination between UAV and UGVs, as well as the communication protocols used for data sharing and decision making.

Section III: System Model provides a detailed description of the system components, including the UAV and UGV models, the hybrid depth sensing model for data acquisition, and the modeling of plant health and disease spread.

Section IV: Proposed Solution outlines the control laws, estimators (WLS and EKF) and algorithms used for data analysis and decision making in the proposed system.

Section V: Implementation details the simulation environment, including the tools and methodologies used to implement the system, and discusses the challenges encountered during the development process.

Section VI: Experimental Results presents numerical and graphical results of the simulations, demonstrating the effectiveness of the proposed system in detecting and responding to plant health problems.

Section VII: Conclusions and Discussion summarises the main findings of the study, discusses the advantages and limitations of the proposed solution, and suggests potential directions for future research.

A. Problem Statement

Precision agriculture has significantly advanced with the adoption of UAV for tasks such as crop health monitoring, land mapping, and disease detection. These technologies have greatly enhanced the ability to gather high-resolution data over large agricultural areas in a short period of time. However, despite these advancements, challenges remain in creating a fully integrated system that can efficiently coordinate aerial and ground-based operations.

While UAV has proven effective in collecting critical data, integrating this data with ground operations, such as those performed by Unmanned Ground Vehicles (UGVs), remains a complex and evolving area. Current systems often face difficulties in integrating data in real-time and coordinating decision-making between UAV and UGVs. For instance, the lack of standardized workflows for combining aerial and ground data can lead to inefficiencies in detecting plant diseases and responding with timely interventions [1], [3].

Additionally, traditional camera-based systems can be limited in their ability to fully capture the complexities of the field environment. Factors such as varying plant heights and dense foliage can obstruct a clear view from above, leading to incomplete or inaccurate data. To address these limitations, a hybrid depth sensing and scanning approach is needed, allowing the system to accumulate data over time and create a comprehensive 3D representation of the field. This method can help overcome the limitations of static imaging and provide a more detailed ground-level assessment.

Moreover, accurately positioning UGVs relative to each other and to the plants is critical for effective operation. Challenges such as sensor noise, environmental variability, and the need for precise navigation in dynamic field conditions necessitate the use of advanced algorithms like Weighted Least Squares (WLS) for accurate positioning and Extended Kalman Filter (EKF) for improved UAV navigation and tracking. These methods help mitigate uncertainties in the data, ensuring that the system can make reliable decisions even under challenging conditions.

In summary, there is a need for more robust and adaptable systems that can efficiently integrate UAV and UGVs, utilizing advanced algorithms like WLS and EKF to enhance data accuracy and decision-making capabilities. These improvements would contribute to more effective monitoring of plant health, allowing for early detection of diseases and better-informed interventions, ultimately leading to more sustainable and productive agricultural practices [6].

II. Distributed System Architecture

In this section, we present the overall architecture of the proposed distributed system, which integrates UAV and UGVs for enhanced plant health monitoring. We discuss the coordination mechanisms between the aerial and ground units, the communication protocols enabling data exchange, and the decision-making processes that allow these platforms to operate in a synchronized and efficient manner across large agricultural fields.

A. UAV and UGV Integration

The integration of UAVs and UGVs is a key component of the distributed system. UAVs fly over the agricultural field,

collecting environmental data using a hybrid depth sensing and scanning model. This model accumulates 3D spatial data as the UAVs move across the field, capturing detailed information about the plants and their surroundings. The data is processed to identify signs of plant disease or stress, and once the inspection is complete, the UAV transmit the data to a central base station for further analysis.

After the analysis, UGVs are deployed to the critical areas identified by the UAV. Equipped with depth sensors similar to those used by the UAV, UGVs autonomously navigate the field, providing detailed ground-level inspections. Their mission includes tasks such as targeted treatments or additional data collection based on the areas identified as problematic by the UAV. The combination of aerial and ground-level data enhances the overall accuracy of the monitoring system.

B. Coordination and Communication

In the proposed system, coordination between UAV and UGVs is managed asynchronously. The UAV first complete his scanning and data collection missions, accumulating detailed 3D spatial data of the agricultural field. This data is then analyzed at a central base station, where it is processed into actionable insights, such as heatmaps that identify areas with a higher probability of disease presence.

Following the analysis, these results are transmitted to the UGVs, which begin their ground-level operations. The UGVs use the processed data to navigate the field, performing tasks such as targeted inspections and interventions based on the UAVs' findings. This approach allows for an efficient division of labor: UAV provides a broad aerial overview, while UGVs conduct more detailed, ground-level work.

Although this project does not focus on the technical details of the communication protocols between UAV and UGVs, it assumes the use of reliable wireless communication methods to facilitate data transfer and coordination. This asynchronous workflow ensures that the system operates efficiently without the need for real-time data sharing, making it suitable for large-scale agricultural monitoring.

C. Distributed Decision-Making

The decision-making process in the system begins with a centralized approach during the initial analysis of data collected by the UAV. Once the UAV completes its data collection and analysis, the instructions are sent to the UGVs. From that point onward, decision-making becomes decentralized. Each UGV operates autonomously, utilizing its local sensors and real-time environmental data to make decisions. This combination of centralized planning and decentralized execution leverages the strength of detailed, global analysis from the UAV while allowing for the adaptability and responsiveness of UGVs on the ground.

III. System Model

This section details the mathematical and technical modeling of the system components, encompassing the UAV and UGV platforms, the hybrid depth sensor and scanning model, and the simulation of plant health and disease propagation within the field. These models provide the foundation for understanding how the system operates in the simulation and how it achieves the objectives of enhanced plant health monitoring and disease detection.

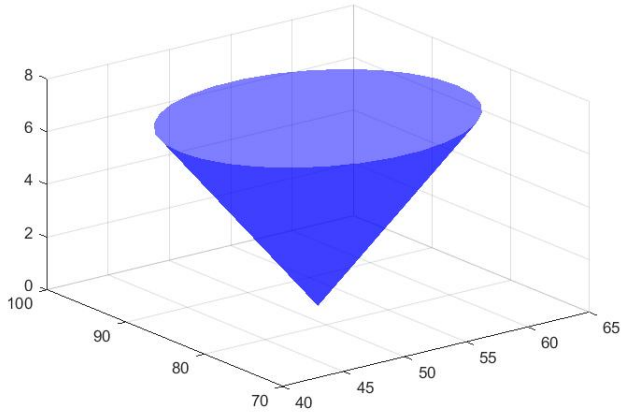

Fig. 2. Cone of vision (UGVs case)

A. UAV and UGV Integration (Technical Description)

In this simulation, both UAV and UGVs are modeled as autonomous agents operating on a unicycle model. The unicycle model describes the vehicle's motion with its state defined by its position (x, y) and orientation θ. This model is well-suited for capturing the dynamics of the UAV and UGVs as they navigate the field.

The unicycle model is represented by the following state equations:

$$\begin{aligned} x_{\text{next}} &= x_{\text{current}} + v \cdot \cos(\theta) \cdot dt, \\ y_{\text{next}} &= y_{\text{current}} + v \cdot \sin(\theta) \cdot dt, \\ \theta_{\text{next}} &= \theta_{\text{current}} + \omega \cdot dt, \end{aligned}$$

where v is the linear velocity, ω is the angular velocity, and dt is the time step used in the simulation.

These equations are implemented in the function `unicicloModel`, which updates the state based on control inputs. Additionally, the function `unicicloJacobian` is used to compute the Jacobian matrices necessary for further state estimation processes.

B. Hybrid Depth Sensor Model

In this system, the UAV and UGVs are equipped with hybrid depth sensors that capture 3D spatial data, surpassing the limitations of traditional 2D imaging. These sensors accumulate depth information over time, enabling the creation of a detailed 3D representation of the environment through active sensing techniques. This approach combines depth perception, akin to that provided by LIDAR or depth cameras, with visual data to produce a more comprehensive model of the field.

The performance of these sensors is governed by several key parameters, including the sensor's height, depth resolution, and

scanning angle. The detection radius r is calculated using an equation similar to that used for a camera's field of view:

$$r = h \cdot \tan\left(\frac{\text{FoV}}{2}\right)$$

where h represents the sensor's height, and FoV denotes the field of view angle:

$$\text{FoV} = 2 \cdot \arctan\left(\frac{W}{2f}\right)$$

Here, W is the sensor width and f is the focal length of the camera. The corresponding field of view in degrees is calculated as:

$$\text{Field of View (degrees)} = \text{rad2deg}\left(\text{FoV}\right)$$

The area covered by the sensor, which is influenced by the detection radius, is given by:

$$\text{Area} = \pi \cdot r^2$$

Additionally, the depth of field (DoF) is computed to determine the range within which objects appear sharp. This is calculated using the following equations:

$$d_{\text{focus}} = \frac{f^2}{N \cdot C} + f$$

where d_{focus} is the focus distance, N is the f-stop, and C is the circle of confusion. The hyperfocal distance H is calculated as:

$$H = \frac{f^2}{N \cdot C}$$

The near and far limits of the depth of field are then given by:

$$d_{\text{min}} = \frac{d_{\text{focus}} \cdot (H - f)}{H + (d_{\text{focus}} - 2f)}$$

$$d_{\text{max}} = \frac{d_{\text{focus}} \cdot (H - f)}{H - (d_{\text{focus}} - 2f)}$$

This hybrid depth sensor model allows the UAV and UGVs to gather data that is then processed into actionable insights, such as identifying areas with higher disease probability or detecting anomalies in plant growth.

1) Camera Parameters: Table II summarizes the key parameters used in the hybrid depth sensor model for both UAV and UGV systems. The values of the parameters are chosen to reflect realistic camera specifications and field conditions, ensuring accurate data collection and analysis.

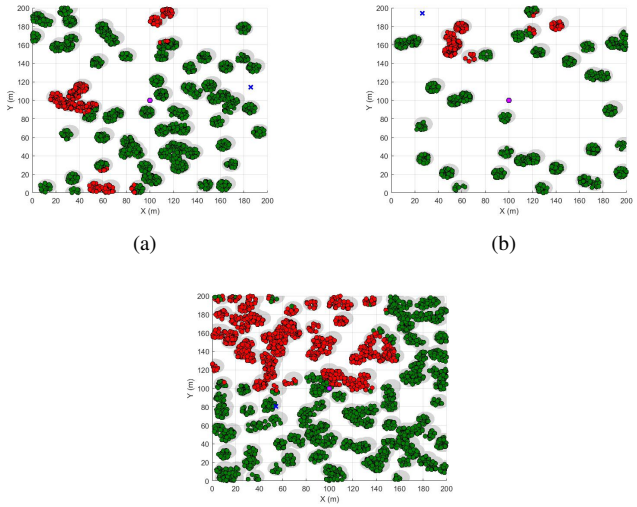

(a) (b)

(c)

Fig. 3. Plant and Disease Modeling: By choosing parameters that describe the field, the plants and the spread of the disease, a wide combination of results can be obtained.

C. Plant and Disease Modeling

The plant and disease models simulate the growth of crops and the progression of diseases within the field. These models incorporate various factors, such as plant biology, environmental conditions, and disease spread dynamics, to create realistic scenarios, as you can see in Fig.3, for the system to monitor. By modeling the health of individual plants and the spread of diseases over time, the system can evaluate different monitoring and intervention strategies.

The plant growth model represents the crops in the field, with individual trees randomly placed within the predefined area. Each tree consists of a number of leaves, with variations in size and position to simulate natural variability. The growth of the trees includes key parameters such as:

- **Tree Canopy:** The radius of the tree canopy and the height of the trees are modeled to simulate the three-dimensional structure of the plants.
- **Leaf Distribution:** Leaves are distributed around the center of each tree, with variability in the number of leaves per tree to reflect realistic growth patterns.
- **Environmental Factors:** Although not explicitly modeled in the current simulation, environmental factors such as light and water can influence future iterations of the growth model.

The disease propagation model simulates how pathogens spread between trees and leaves within the field. The process begins with a few initially infected trees, and the disease then spreads to nearby leaves and plants based on proximity and specific conditions:

- **Initial Infection:** A small subset of trees is randomly selected as initially infected. The leaves of these trees are immediately marked as infected.
- **Infection Spread:** The disease spreads from infected leaves to healthy leaves based on the distance between them. The probability of infection is influenced by the

relative height of the leaves, with a higher likelihood of infection spreading downward. Infected leaves can spread the disease within a defined radius, simulating realistic contagion dynamics in the field.

- **Probabilistic Infection:** The likelihood of infection is determined by factors such as proximity and height difference. For example, the disease is more likely to spread to lower leaves, while the spread to higher leaves is less probable.

The system also includes parameters for visualizing and tracking the spread of the disease. Healthy and infected leaves are stored separately, allowing for further analysis and intervention. This enables the UAV and UGV systems to detect early signs of disease and adjust their strategies to prevent widespread outbreaks.

IV. Proposed Solution

In this section, we describe the control strategies, estimators, and algorithms developed to enhance the performance of the distributed UAV-UGV system. We specifically focus on the application of Weighted Least Squares (WLS) for managing positional uncertainties and the Extended Kalman Filter (EKF) for improving the accuracy of UAV navigation. Additionally, we discuss the image processing and decision-making algorithms that enable the system to detect plant diseases early and optimize intervention strategies.

A. Control Laws

The control laws govern the movement and behavior of both the UAV and UGVs as they navigate through the agricultural field.

a) UAV Control Laws: The UAV control laws manage stable flight, waypoint navigation, and coverage optimization. The function `calcolaComandiControllo` dynamically adjusts the UAV's angular gain and speed based on the distance to the waypoint, ensuring that the UAV maintains the appropriate altitude and velocity to capture high-quality images. The control logic also incorporates constraints to avoid excessive angular velocities, ensuring smooth flight operations.

The linear velocity v and angular velocity ω are calculated using the following formulas:

$$\begin{aligned} v &= \begin{cases} v_{\max} \cdot \frac{d_{\text{wayp.}}}{d_{\text{dec.}}}, & \text{if } d_{\text{wayp.}} < d_{\text{dec.}} \\ v_{\min} + (v_{\max} - v_{\min}) \cdot \text{scale factor}, & \text{otherwise} \end{cases} \\ \omega &= \text{clamp}\left(K_p \cdot \text{error}, \omega_{\min}, \omega_{\max}\right) \end{aligned} \tag{1}$$

Here, $d_{\text{wayp.}}$ is the distance to the waypoint, and $d_{\text{dec.}}$ is the distance at which deceleration begins. The angular gain Kp is dynamically adjusted based on the distance to the waypoint, providing a smooth and accurate approach.

b) UGV Control Laws: For UGVs, the control laws focus on ground navigation and obstacle avoidance. The function `calcolaComandiControlloUGV` computes the UGV's velocity and angular velocity based on the current state, waypoint, and collision avoidance mechanisms. The UGV control logic incorporates several layers of decision-making to ensure safe navigation, including adjustments for proximity to obstacles such as trees and other UGVs.

The control commands for UGVs are determined as follows:

$$v = v_{\min} + (v_{\max} - v_{\min}) \cdot \min\left(\frac{d_{\text{waypoint}}}{d_{\text{threshold}}}, 1\right)$$

$$\omega = Kp_{\text{angolo}} \cdot \text{errore\_angolo} - \sum_i \left(\text{sign}(\text{angolo\_differenza}) \cdot \omega_{\max}\right)$$

The angular velocity ω is adjusted not only based on the waypoint but also in response to nearby obstacles, ensuring collision avoidance. The term $\sum_i \left(\text{sign}(\text{angolo\_differenza}) \cdot \omega_{\max}\right)$ accounts for adjustments needed to avoid collisions with other UGVs or trees, where angolo_differenza is the angular difference between the UGV's heading and the direction of the obstacle.

B. Estimators

Estimators are essential for handling uncertainties and improving the accuracy of data collected by the UAV and UGVs. Two key estimators used in this system are the Extended Kalman Filter (EKF) and Weighted Least Squares (WLS).

1) EKF: The Extended Kalman Filter (EKF) is used primarily for UAV state estimation, combining GPS and IMU data to provide continuous and accurate estimates of the UAV's position and orientation. The function `stimaEKF` performs the prediction and update steps of the EKF, utilizing the UAV's motion model and incorporating both process noise and measurement noise covariances to refine the state estimates.

The EKF algorithm follows two main phases: prediction and update.

Prediction Phase:

$$\hat{x}_{k|k-1} = f(\hat{x}_{k-1}, u_k)$$

$$P_{k|k-1} = F_k P_{k-1} F_k^T + Q$$

Update Phase (GPS and IMU):
For the GPS:

$$K_{\text{GPS}} = P_{k|k-1} H^T (H P_{k|k-1} H^T + R_{\text{GPS}})^{-1}$$

$$\hat{x}_k = \hat{x}_{k|k-1} + K_{\text{GPS}}(z_{\text{GPS}} - H\hat{x}_{k|k-1})$$

$$P_k = (I - K_{\text{GPS}} H) P_{k|k-1}$$

For the IMU:

$$K_{\text{IMU}} = P_{\text{GPS}} H^T (H P_{\text{GPS}} H^T + R_{\text{IMU}})^{-1}$$

$$\hat{x}_k = \hat{x}_{\text{GPS}} + K_{\text{IMU}}(z_{\text{IMU}} - H\hat{x}_{\text{GPS}})$$

$$P_k = (I - K_{\text{IMU}} H) P_{\text{GPS}}$$

These equations describe how the EKF combines data from GPS and IMU sensors to estimate the UAV's state.

a) Integration of IMU Angular Velocity in the EKF: In the UAV simulation, the Extended Kalman Filter (EKF) has been enhanced by integrating the IMU's angular velocity (ω_{imu}) directly into the system's state model, rather than using a direct orientation measurement (z_{imu}) in the update phase. This approach simplifies the process and improves the robustness of the orientation estimate.

State Model and Prediction: Instead of a separate update for the IMU, the angular velocity is used in the prediction step:

$$\theta_{t+1} = \theta_t + \omega_{imu} \cdot \Delta t$$

This modification streamlines the EKF by embedding the IMU's data directly into the motion model, eliminating the need for an additional update step.

IMU Noise Covariance: The traditional IMU noise covariance (R_{imu}) is incorporated into the process noise covariance matrix (Q) rather than being used in a separate update step. This adjustment reflects the overall uncertainty of the state model:

$$Q = \text{diag}(q_x, q_y, \sigma_\omega)^2$$

This method improves the accuracy and stability of the UAV's state estimation, particularly in environments with high noise levels.

2) WLS: WLS is employed by the UGVs to refine position estimates based on shared data from other UGVs. The function `WLS` aggregates position estimates from multiple UGVs, weighting them according to the confidence in each measurement.

The WLS estimator is defined as:

$$\hat{x}_{\text{WLS}} = \frac{\sum_{i=1}^{n} w_i x_i}{\sum_{i=1}^{n} w_i}$$

where:

- $\hat{x}_{\text{WLS}}$ is the final weighted estimate,
- w_i is the weight associated with the estimate x_i.

This approach reduces the uncertainty in the UGV's position estimates and enables better coordination among the UGVs by considering the reliability of the data collected from each vehicle.

C. Algorithms for Image Processing

The image processing algorithms enable the UAV to detect plant diseases using the hybrid depth sensors that collect both visual and spatial data. Techniques such as image segmentation, feature extraction, and depth-based anomaly detection are applied to identify patterns indicative of plant stress or disease. Unlike a traditional pinhole camera model, the hybrid sensor model accumulates 3D spatial information over time, allowing for a more comprehensive analysis of the environment.

These sensors capture depth data that is used to create detailed topographic maps of the field, which are then processed to generate heatmaps. These heatmaps visually represent areas with a higher probability of disease presence, guiding the UGVs to the most critical locations for targeted interventions. This approach enhances the precision of the disease detection process by leveraging both visual and spatial information to identify subtle changes in plant health.

D. Decision-Making Algorithms

The decision-making algorithms guide the actions of both UAV and UGVs based on the hybrid sensor data collected and processed. For the UAV, these algorithms determine the next waypoints for further exploration based on the coverage achieved and the areas identified as potentially problematic, leveraging the 3D maps created from accumulated spatial data.

For UGVs, the decision-making process involves selecting which areas to inspect or treat based on the 3D heatmaps and spatial models generated by the UAV. These algorithms prioritize locations with a higher probability of disease presence, optimizing the UGVs' routes to minimize travel time and energy consumption while ensuring thorough coverage of the field. The hybrid sensor data allows UGVs to make more informed decisions, considering both the visual and topographical information in their path planning and intervention strategies.

V. Implementation

This section details the implementation of the proposed system within a simulation environment. We describe the tools and software used, the integration of the UAV and UGV models, and the process of simulating the unsynchronized communication and data processing within the distributed system. Additionally, pseudocode is provided to illustrate the core algorithms implemented in the simulation, offering a clearer understanding of the system's functionality.

A. Simulation Environment

The simulation environment serves as a virtual testbed where the UAV and UGV systems, along with various algorithms and estimators, are modeled and evaluated. MATLAB is used as the primary and unique platform for the simulation, providing tools for modeling dynamic systems, processing spatial and visual data, and visualizing the results.

The UAV and UGVs are equipped with hybrid depth sensors that collect spatial data over time, enabling the generation of detailed 3D maps of the agricultural field. The simulation environment includes a representation of the field, where trees and plants are randomly positioned, and the spread of disease is simulated to create realistic scenarios. These hybrid sensors accumulate data from multiple positions, allowing for the creation of a comprehensive map that guides the ground-level operations of the UGVs.

The environment also supports 3D visualization, enabling the monitoring of UAV and UGV performance as they explore the field and respond to detected issues. The ability to visualize both spatial and visual data in real time enhances the understanding of the system's effectiveness in managing plant health and disease detection.

B. System Integration

The integration of UAV and UGV systems within the simulation environment is crucial to the overall functionality of the project. This involves combining the individual models, algorithms, and hybrid depth sensors into a cohesive system capable of autonomously operating in a coordinated manner.

The hybrid depth sensors integrated into the UAVs and UGVs play a pivotal role in improving the quality of data collected during the simulation. These sensors allow the UAVs to capture both visual and spatial data, which is then processed into detailed 3D maps of the field. The data collected by the UAVs is communicated to the UGVs, guiding them to the critical areas identified by the aerial scans. The UGVs, equipped with the WLS estimator, refine their position estimates based on this spatial data, ensuring precise navigation and obstacle avoidance.

The following pseudocode outlines the process of integrating the EKF, WLS, and hybrid camera models within the simulation environment.

1) Extended Kalman Filter (EKF) Integration: The EKF is crucial for UAV state estimation, combining GPS and IMU data to provide accurate estimates of the UAV's position and orientation. The pseudocode Algorithm 1 illustrates the EKF implementation:

Algorithm 1 EKF_Update

Input: Current state estimate x_{est}, Covariance matrix P, Control input u, GPS measurement z_{gps}, IMU measurement ω_{imu}
Output: Updated state estimate $x_{est\_updated}$, Updated covariance matrix $P_{updated}$
Predict the next state using the Unicycle Model:
  $u_{pred} = [u(1); \omega_{imu}]$
  $x_{pred} = \text{UnicycleModel}(x_{est}, u_{pred}, dt)$
  $[F, G] = \text{UnicycleJacobian}(x_{est}, u_{pred}, dt)$
  $P_{pred} = F \cdot P \cdot F^T + G \cdot Q \cdot G'$
GPS Update Phase:
  $H_{gps} = [1\ 0\ 0;\ 0\ 1\ 0]$
  $y_{gps} = z_{gps} - H_{gps} \cdot x_{pred}$
  $S_{gps} = H_{gps} \cdot P_{pred} \cdot H_{gps}^T + R_{gps}$
  $K_{gps} = P_{pred} \cdot H_{gps}^T / S_{gps}$
  $x_{est\_updated} = x_{pred} + K_{gps} \cdot y_{gps}$
  $P_{updated} = (I - K_{gps} \cdot H_{gps}) \cdot P_{pred}$
Ensure orientation angle is within $[-\pi, \pi]$
Return $x_{est\_updated}$, $P_{updated}$

2) Weighted Least Squares (WLS) Integration: The WLS algorithm is employed by the UGVs to refine their position estimates based on shared data from other UGVs. The pseudocode Algorithm 2 outlines the WLS estimation process:

3) Camera Data Processing Integration: The hybrid camera system collects 3D spatial data, which is processed to create detailed maps of the agricultural field. The pseudocode Algorithm 3 outlines the camera data processing:

C. Challenges and Solutions

During the implementation of the simulation, several challenges were encountered, particularly related to the integration of spatial data from the hybrid depth sensors and the overall system coordination.

Algorithm 2 WLS_Estimation

Input: Position estimates from UGVs $ugv\_positions$, Weights $ugv\_weights$, Shared data $condivisi\_dati$
Output: Updated position estimates $ugv\_estimated\_positions$
for each UGV i **do**
  $aggregated\_estimate = ugv\_weights[i] \cdot ugv\_positions[i]$
  $total\_weight = ugv\_weights[i]$
  for each other UGV $j \neq i$ **do**
    $aggregated\_estimate+ = condivisi\_dati[j].weight \cdot condivisi\_dati[j].position$
    $total\_weight+ = condivisi\_dati[j].weight$
  end for
  $ugv\_estimated\_positions[i] = aggregated\_estimate/total\_weight$
end for
Return $ugv\_estimated\_positions$

Algorithm 3 CameraDataProcessing

Input: Camera parameters (height, focal length, sensor width, etc.), Position of UAV/UGV
Output: 3D maps of the field, Depth and visual data
Calculate Field of View (FoV) and detection radius:
  $\theta = 2 \cdot atan(W/(2 \cdot f))$
  $raggio\_rilevazione = height \cdot tan(\theta/2)$
Calculate Depth of Field (DoF) based on camera parameters:
  $d\_focus = (f^2)/(N \cdot C) + f$
  $H = (f^2)/(N \cdot C)$
  $d\_min = (d\_focus \cdot (H - f))/(H + (d\_focus - 2 \cdot f))$
  $d\_max = (d\_focus \cdot (H - f))/(H - (d\_focus - 2 \cdot f))$
Generate 3D map:
for each position (x, y) in the field **do**
  Capture depth data and visual data
  Update 3D map with new data
end for
Return 3D maps, Depth data, Visual data

a) Handling Spatial Data from Hybrid Sensors: One of the main challenges was efficiently processing the spatial data collected by the hybrid sensors, particularly in ensuring that the heatmaps generated were accurate and actionable for UGV operations. This involved refining the methods used to integrate and interpret the data collected over time by the UAV and UGV systems, ensuring that the resulting maps were detailed and precise enough to guide ground operations effectively.

b) Handling Sensor Noise and Data Uncertainty: Another challenge involved managing the uncertainties and noise in the sensor data, particularly for UAV navigation and UGV ground operations. The use of the EKF for UAV state estimation and WLS for UGV position refinement was crucial in addressing these issues. These methods allowed the system

to maintain accurate tracking and positioning even when the sensor data was imperfect, ensuring reliable operation under varying conditions.

c) Obstacle Avoidance and Collision Prevention: In the UGV operations, ensuring that the vehicles could navigate the field without colliding with trees or other UGVs was a key challenge. This was managed by implementing advanced control algorithms that incorporated real-time sensor data to adjust the UGV's path and avoid obstacles while still moving toward the target locations. Additionally, determining appropriate parameters, such as the minimum distance to be kept from trees, required careful consideration of environmental characteristics, including the density and size of trees in the field.

d) Heatmap Accuracy: Generating accurate heatmaps based on the hybrid sensor data was another challenge. The data collected from the aerial perspective had to be processed and translated into actionable information for the UGVs, considering both the visual and spatial aspects. Refining the image processing algorithms and adjusting the parameters of the hybrid sensors helped improve the resolution and accuracy of the disease detection process, leading to more precise UGV interventions.

VI. Experimental Results

In this section, we present and analyze the results of the simulations conducted to evaluate the performance of the proposed system. We provide both numerical and graphical data to demonstrate the system's effectiveness in detecting plant diseases, its accuracy in UAV navigation, and the overall impact on agricultural management. The results are discussed in the context of their implications for real-world applications and future improvements.

A. Simulation Setup

The simulations were conducted in a controlled virtual environment, with specific parameters consistent across all scenarios. These include the size of the agricultural field, the number of trees, and the UAV and UGV characteristics. However, certain variables were adjusted across simulations to assess the system's robustness under different conditions. The primary variables modified include sensor noise levels and camera parameters. The performance of the system was evaluated based on metrics such as disease detection accuracy, navigation precision, and operational efficiency.

From the table I, we can see the parameters used in the simulation setup.

B. Simulation 1: Baseline

The baseline simulation was performed under standard conditions, with default sensor settings and minimal noise interference. The results of this simulation serve as a reference for evaluating the impact of altered conditions in subsequent simulations. Key performance indicators, such as the accuracy of disease detection and the stability of UAV navigation, were recorded and analyzed.

The results obtained from the simulation are plotted and shown in the following Figures: 4,5, 6, 7 and 8. It is possible to observe the route travelled by the drones and their trajectories, the heatmaps, the IDs of the trees, the submaps required for the UGVs and the list and location of the various trees searched by the UAV using an ID.

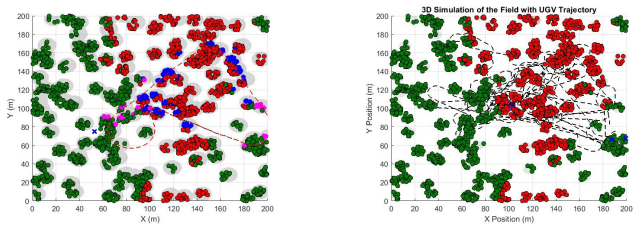

(a) (b)

Fig. 4. UAV and UGV perlustration of the field

C. Simulation 2: Increased Sensor Noise

In this simulation, the noise levels in the UAV and UGV sensors were significantly increased to evaluate the system's robustness under high uncertainty conditions. Specifically, the parameters related to sensor noise, such as the sigma values

TABLE I
SIMULATION SETUP PARAMETERS

Parameter	Value	Description
Field Size	200 m x 200 m	Dimensions of the agricultural field
Total Area	40,000 m^2	Total area of the field
Number of Trees	80	Number of trees randomly distributed in the field
UAV Flight Height	7 m	Altitude at which the UAV operates
UAV Minimum Speed	4 m/s	Minimum linear velocity of the UAV
UAV Maximum Speed	10 m/s	Maximum linear velocity of the UAV
UAV Angular Velocity	0.5 - 1 rad/s	Range of angular velocity for the UAV
UGV Camera Height	1 m	Height of the camera on the UGV
UGV Minimum Speed	1 m/s	Minimum linear velocity of the UGV
UGV Maximum Speed	7 m/s	Maximum linear velocity of the UGV
Tree Canopy Radius	5 m	Radius of the tree canopy
Max Tree Height	3 m	Maximum height of the trees in the field
Initial Infected Trees	4	Number of trees initially infected with the disease
Disease Spread Radius	20 m	Radius within which the disease can spread from an infected tree
Percentage of Field to Explore	30%	Proportion of the field that the UAV must cover during the exploration phase

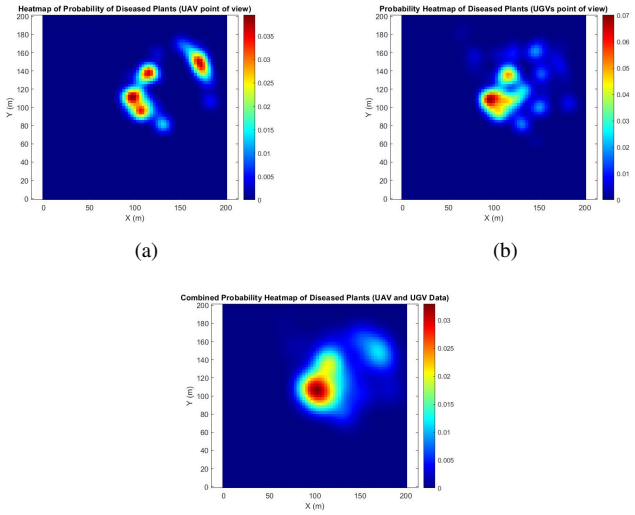

(a) (b) (c)

Fig. 5. Heatmaps generated by the simulation

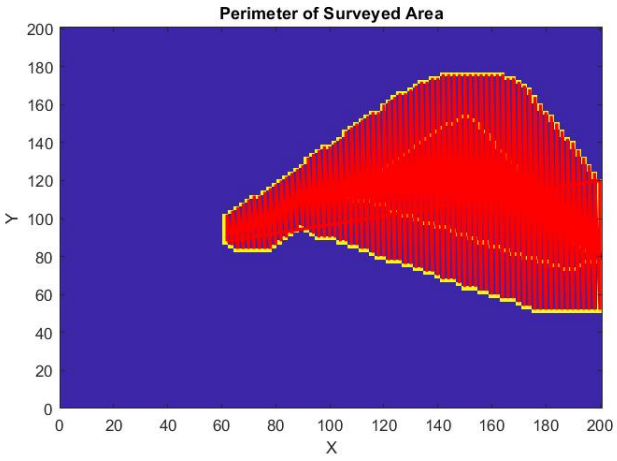

Fig. 6. Perlustrated field from UAV

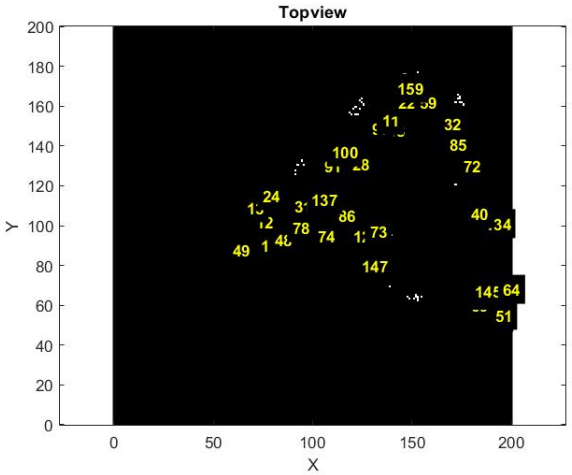

Fig. 7. ID of the trees

for GPS, IMU, and camera uncertainties, were augmented. The goal was to observe how this increased noise affects the system's performance, particularly in terms of UAV stability, UGV navigation accuracy, and the reliability of disease detection. Please, take a look at Table III.

During the simulation, the effects of heightened sensor noise were closely monitored, including potential delays in response, miscalculations in positioning, and overall system stability. By comparing these results with the baseline simulation, we were able to quantify the performance degradation and identify the critical points where the system's functionality started to decline due to excessive noise.

The results are showed in the Fig. 9

D. Simulation 3: Extreme Sensor Uncertainty

In the third simulation, we further escalated the sensor uncertainty parameters to extreme levels to test the system's breaking points, as you can see from Table IV. This involved not only increasing the noise levels but also modifying the uncertainty factors related to the UAV's and UGV's field of view and detection capabilities. The aim was to assess how extreme levels of uncertainty would impact the system's ability to function effectively, particularly in detecting plants, navigating the field, and avoiding obstacles.

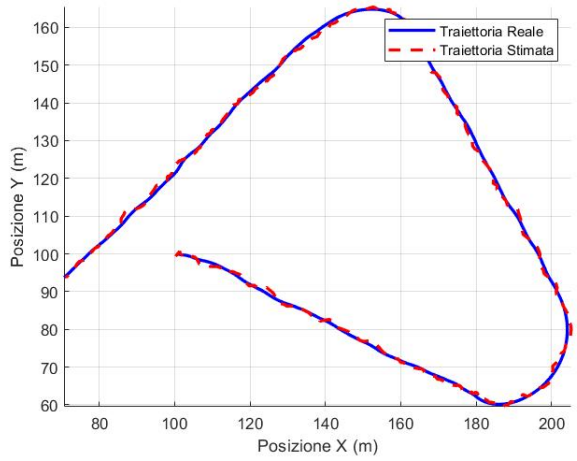

Fig. 8. Real and estimated trajectory of the UAV

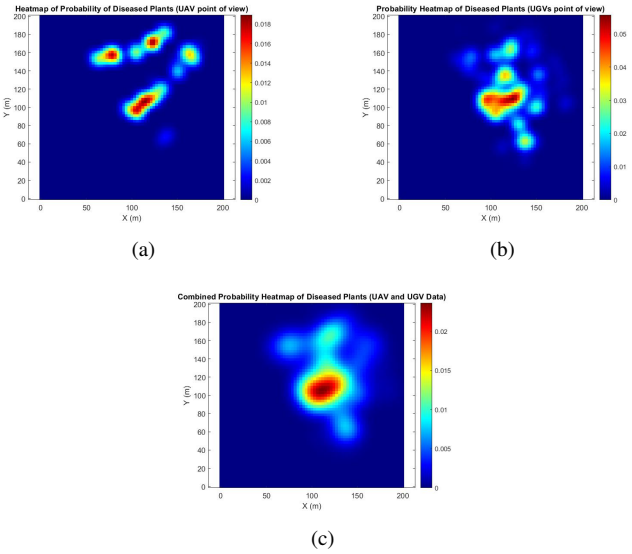

(a) (b)

(c)

Fig. 9.

As a result of these extreme conditions, significant alterations in the UAV's and UGV's vision cones were observed. The UAV's vision cone became significantly narrower, while the UGV's expanded beyond its normal range, leading to challenges in accurately detecting leaves and maintaining a consistent path. In some cases, the UAV or UGV failed to identify crucial waypoints or targets, which highlighted the limitations of the system when operating under excessively uncertain conditions. This simulation emphasized the importance of optimizing sensor parameters to maintain a balance between robustness and precision, avoiding scenarios where the system's effectiveness is severely compromised.

The results are showed in the Fig. 10

VII. Conclusion

This study effectively implemented and simulated a distributed UAV-UGV system designed for precision agriculture. Through various simulation scenarios, the system's performance was evaluated in areas such as UAV navigation accuracy, UGV obstacle avoidance, and plant disease detection. A key finding was the significant impact of sensor uncertainties on system functionality. As uncertainty parameters like sigma values and other factors increased, there were noticeable changes in the cones of vision for both UAV and UGVs—narrowing for UAV and widening for UGVs. This adaptability allowed the system to maintain reliability under different uncertainty conditions.

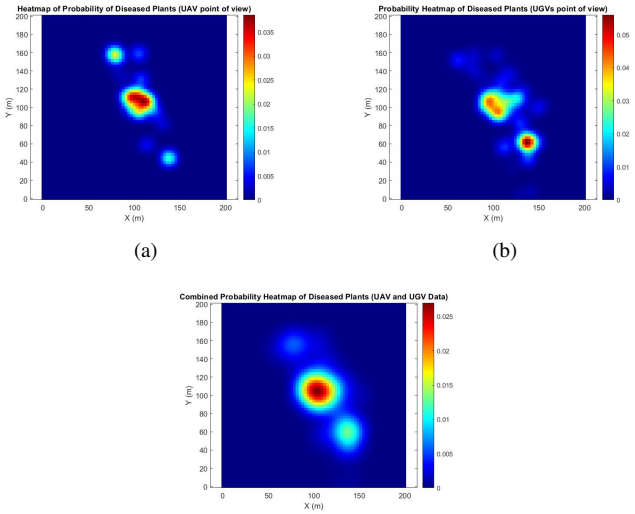

(a) (b)

(c)

Fig. 10.

However, when uncertainty parameters were excessively increased, the system's performance began to degrade. The cones of vision became so distorted that crucial environmental details, such as leaves or waypoint markers, were missed. In extreme cases, this led to the UAV or UGV failing to detect key targets, compromising their monitoring and intervention capabilities. This trade-off emphasizes the importance of carefully tuning sensor uncertainty parameters to balance robustness and accuracy. While the system shows strong adaptability, it is crucial to optimize the management of sensor uncertainties to prevent significant performance degradation.

The findings suggest that, while the proposed system holds considerable promise for enhancing precision agriculture, further refinements are needed, particularly in the calibration of sensor uncertainties, to ensure effective operation across diverse environmental conditions.

References

[1] D. C. Tsouros, S. Bibi, and P. G. Sarigiannidis, "A review on uav-based applications for precision agriculture," *Information*, vol. 10, no. 11, p. 349, 2019. [Online]. Available: https://www.mdpi.com/2078-2489/10/11/349

[2] G. Grenzdörffer and J. Chen, "Advances of uav in precision agriculture," *Drones*, vol. 8, no. 1, 2024, special Issue. [Online]. Available: https://www.mdpi.com/journal/drones/special_issues/UAV_Precision_Agriculture

[3] M. Herrero-Huerta, J. A. Jiménez-Berni, S. Sun, I. Herrmann, and D. González-Aguilera, "Unmanned ground and aerial vehicles (ugvs-uavs) for digital farming," *MDPI Topics*, 2024. [Online]. Available: https://www.mdpi.com/topics/UGVs-UAVs_for_Digital_Farming

[4] “Plant disease detection using drones in precision agriculture,” *Precision Agriculture*, 2023, accessed August 2023. [Online]. Available: https://link.springer.com/article/10.1007/s11119-023-09879-2

[5] R. Zhang, A. Hewitt, and A. Tofael, “Recent advances in crop protection using uav and ugv,” *Drones*, vol. 8, 2024. [Online]. Available: https://www.mdpi.com/journal/drones/special_issues/Recent_Advances_Crop_Protection_UAV_UGV

[6] P. Tokekar, J. V. Hook, D. Mulla, and V. Isler, “Trends in development of uav-ugv cooperation approaches in precision agriculture,” *SpringerLink*, 2023. [Online]. Available: https://link.springer.com/article/10.1007/s11119-023-09879-2

TABLE II
CAMERA PARAMETERS FOR UAV AND UGV SYSTEMS

Parameter	Value	Description
UAV Height (altezza_uav)	7 m	UAV flight altitude
Focal Length (f_uav)	0.012 m	Camera focal length for UAV
Sensor Width (W_uav)	0.036 m	Camera sensor width for UAV
f-stop (N)	4	Aperture (f-stop) of the camera
Circle of Confusion (C)	0.03 m	Acceptable circle of confusion
Field of View (FoV)	114.6°	Field of view angle of the camera
Minimum Focus Distance (d_min)	Calculated	Nearest point in focus (depends on focal length, aperture, and focus distance)
Maximum Focus Distance (d_max)	Calculated	Furthest point in focus (depends on focal length, aperture, and focus distance)

TABLE III
COMPARISON OF PARAMETERS FOR SIMULATION 2

Parameter	Initial Value (UAV)	New Value (Simulation 2, UAV)	Initial Value (UGV)	New Value (Simulation 2, UGV)
Sigma for UAV Height ($\sigma\_altezza$)	0.1	0.3	N/A	N/A
Sigma for Focal Length (σ_f)	0.001	0.003	N/A	N/A
Sigma for Sensor Width (σ_W)	0.001	0.003	N/A	N/A
Uncertainty Factor for Distance (fattore_distanza)	0.03	0.06	0.1	0.3
Uncertainty Factor for Visibility (fattore_visibilita)	1.0	1.5	1.5	2
Uncertainty Factor for Height (fattore_altezza)	0.03	0.06	0.05	0.1
Occlusion Radius (raggio_oscuramento)	8 m	8 m	8 m	8 m

TABLE IV
COMPARISON OF PARAMETERS FOR SIMULATION 3

Parameter	Initial Value (UAV)	New Value (Simulation 3, UAV)	Initial Value (UGV)	New Value (Simulation 3, UGV)
Sigma for UAV Height ($\sigma\_altezza$)	0.3	0.8	N/A	N/A
Sigma for Focal Length (σ_f)	0.003	0.008	N/A	N/A
Sigma for Sensor Width (σ_W)	0.003	0.008	N/A	N/A
Uncertainty Factor for Distance (fattore_distanza)	0.06	0.2	0.3	0.9
Uncertainty Factor for Visibility (fattore_visibilita)	1.5	2.5	2	3
Uncertainty Factor for Height (fattore_altezza)	0.06	0.15	0.1	0.5
Occlusion Radius (raggio_oscuramento)	8 m	8 m	8 m	8 m